

# Soliton trapping in fiber lasers

L. M. Zhao<sup>1,\*</sup>, D. Y. Tang<sup>1</sup>, H. Zhang<sup>1</sup>, X. Wu<sup>1</sup>, and N. Xiang<sup>2</sup>

<sup>1</sup> School of Electrical and Electronic Engineering, Nanyang Technological University, Singapore, 639798

<sup>2</sup> Center for Optoelectronics, Department of Electrical and Computer Engineering, National University of Singapore, Singapore, 117576

\*Corresponding author: [lmzhao@ntu.edu.sg](mailto:lmzhao@ntu.edu.sg)

**Abstract:** We report on the soliton trapping in a fiber ring laser mode-locked with a SESAM. It was observed that solitons along the two orthogonal polarization directions of the cavity with fairly large difference in central frequency and energy could be coupled together to form a group velocity locked vector soliton. In particular, due to that each of the coupled solitons forms its own soliton sidebands, two sets of soliton sidebands could be observed on the vector soliton spectrum. Numerical simulations have well confirmed the experimental observations.

©2008 Optical Society of America

**OCIS codes:** 060.4370 (Nonlinear optics, fibers); 060.5530 (Pulse propagation and temporal solitons); 140.3510 (Lasers, fiber).

---

## References and links

1. C. R. Menyuk, "Stability of solitons in birefringent optical fibers. I: Equal propagation amplitudes," *Opt. Lett.* **12**, 614-616 (1987).
2. C. R. Menyuk, "Stability of solitons in birefringent optical fibers. II. Arbitrary amplitudes," *J. Opt. Soc. Am. B* **5**, 392-402 (1988).
3. M. N. Islam, C. D. Poole, and J. P. Gordon, "Soliton trapping in birefringent optical fibers," *Opt. Lett.* **14**, 1011-1013 (1989).
4. E. Korolev, V. N. Nazarov, D. A. Nolan, and C. M. Truesdale, "Experimental observation of orthogonally polarized time-delayed optical soliton trapping in birefringent fibers," *Opt. Lett.* **30**, 132-134 (2005)
5. S. M. J. Kelly, "Characteristic sideband instability of periodically amplified average soliton," *Electron. Lett.* **28**, 806-807 (1992).
6. S. Cundiff, B. Collings, and W. Knox, "Polarization locking in an isotropic, modelocked soliton Er/Yb fiber laser," *Opt. Express* **1**, 12-21 (1997).
7. B. C. Collings, S. T. Cundiff, N. N. Akhmediev, J. M. Soto-Crespo, K. Bergman, and W. H. Knox, "Polarization-locked temporal vector solitons in a fiber laser: experiment," *J. Opt. Soc. Am. B* **17**, 354-365 (2000).
8. S. T. Cundiff, B. C. Collings, and K. Bergman, "polarization locked vector solitons and axis instability in optical fiber," *Chaos*, **10**, 613-624 (2000).
9. D. Y. Tang, L. M. Zhao, B. Zhao, and A. Q. Liu, "Mechanism of multisoliton formation and soliton energy quantization in passively mode-locked fiber lasers," *Phys. Rev. A* **72**, 043816 (2005).
10. N. N. Akhmediev, A. Ankiewicz, M. J. Lederer, and B. Luther-Davies, "Ultrashort pulses generated by mode-locked lasers with either a slow or a fast saturable-absorber response," *Opt. Lett.* **23**, 280-282 (1998).

---

## 1. Introduction

Soliton trapping in optical fibers was first theoretically predicted by Curtis R. Menyuk [1, 2]. It refers to as the phenomenon that two solitons formed along each of the two orthogonal polarization directions of a weakly linear birefringent fiber can trap each other and co-propagate as a non-dispersive unit despite of their intrinsic group velocity difference. Such a unit of coupled solitons was also known as a group velocity locked vector soliton (GVLVS). It was shown that such a vector soliton could be formed because the two solitons shifted their central frequencies in opposite directions through the self-phase modulation and cross-phase modulation. Soliton trapping effect in optical fibers has been experimentally demonstrated [3, 4].

Optical solitary waves can also be formed in fiber lasers. However, different from the solitons formed in fibers, solitons formed in a laser are dissipative in nature. Their formation is due to the mutual interaction among the cavity dispersion, fiber nonlinear Kerr effect,

cavity gain and losses, as well as the cavity boundary condition. In particular, because of the periodic discrete perturbations of the cavity components, soliton sidebands are formed on their optical spectrum [5]. Both theoretical and experimental studies on the soliton sidebands have shown that their appearance is pair-wise symmetric to the soliton peak frequency, and their positions on the soliton spectrum are only the soliton parameters and the net cavity dispersion dependent.

Except the polarization maintaining fiber being used, generally speaking, the cavity of a fiber laser is weakly birefringent. Therefore, soliton generation and propagation in a fiber laser cavity are always subjected to the influence of the cavity birefringence. For soliton fiber lasers mode-locked with the nonlinear polarization technique, because a polarizer is inserted in the cavity for achieving the artificial saturable absorption effect, and it defines the soliton polarization at the cavity position, no vector solitons could be formed in the fiber lasers. The situation is completely changed for soliton fiber lasers mode-locked with a semiconductor saturable absorber mirror (SESAM). S. T. Cundiff et al. have shown with a linear cavity fiber laser that both the GVLVS and the phase locked vector solitons (PLVS) could be formed in the lasers [6]. In particular, they have shown that a PLVS could maintain its polarization during propagation in the cavity, while a GVLVS is characterized by its polarization rotation during the propagation. Therefore, a GVLVS also exhibited a “polarization evolution frequency (PEF)” in the RF spectrum when measured after an external cavity polarizer, while no PEF for the PLVS solitons [6]. Furthermore, Cundiff et al. have also reported the observation of “polarization sidebands” on the optical spectra of the GVLVSs. These sidebands are different from the conventional soliton sidebands by that their positions are the cavity birefringence dependent. However, in Cundiff et al.’s experiments all the vector solitons have only single set of soliton sidebands [6-8].

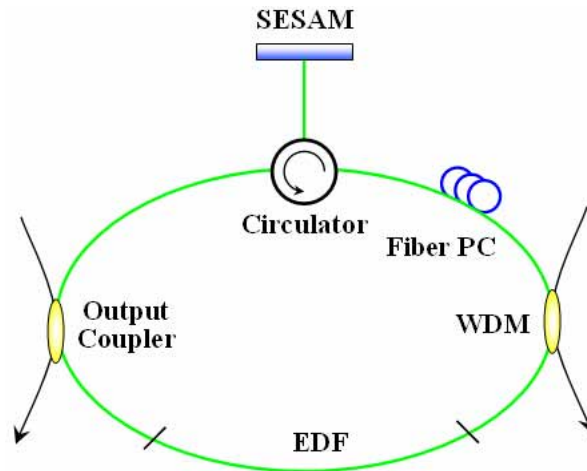


Fig. 1. Schematic of the fiber laser. SESAM: semiconductor saturable absorber mirror; PC: polarization controller; WDM: wavelength-division multiplexer; EDF: erbium-doped fiber.

In this paper we report on the experimental observation of another type of GVLVS in the passively mode-locked fiber lasers. We show that even with moderate linear cavity birefringence, GVLVSs could still be formed in a fiber laser. However, due to that the two orthogonally polarized solitons have large central frequency and energy difference, two sets of soliton sidebands appear on the vector soliton.

## 2. Experimental setup

A schematic of our fiber laser is shown in Fig. 1. The laser has a ring cavity, which consists of 2.63 m erbium-doped fiber (StockerYale EDF-1480-T6), 2.97 m standard single mode fibers (SMFs), a 3-port polarization independent circulator and a SESAM. The circulator has the function of incorporating the SESAM in the cavity and simultaneously forcing the

unidirectional operation of the laser. A 1480 nm Raman fiber laser with maximum output of 220 mW was used to pump the laser. To avoid CW overdriving of the SESAM by the residual pump power, the pump beam was coupled into the cavity with the reverse-pumping scheme. The laser output was through a 10% fiber coupler. A fiber-based polarization controller was inserted in the cavity to control the net cavity birefringence. The SESAM used has a saturable absorption of 8%, and a recovery time of 2 ps. The fiber length between the circulator and the SESAM was 0.4 m.

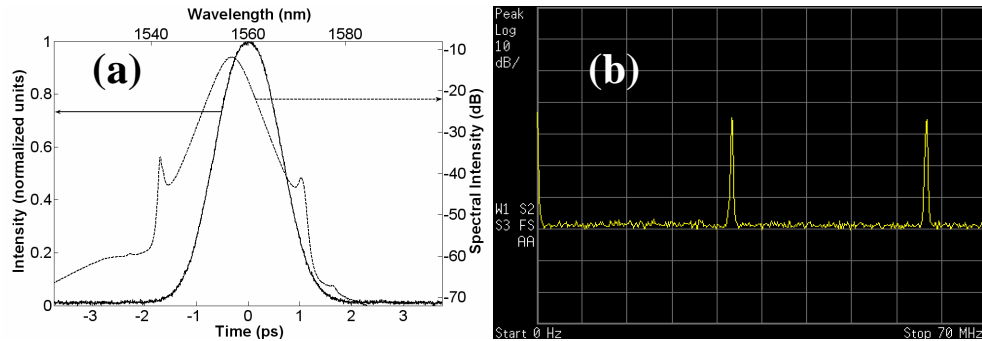


Fig. 2. A typical vector soliton experimentally obtained. (a) Optical spectrum and the corresponding autocorrelation trace; (b) RF spectrum after an external linear polarizer.

### 3. Experimental results

As no explicit polarization discrimination components were used, and all the fibers used have weakly birefringence, vector solitons were always observed. In our laser we could observe all the phenomena reported by Cundiff et al regarding the polarization dynamics of vector solitons. Figure 2 shows for example a typical case of the PLVS operation of the laser. Figure 2(a) shows the optical spectrum and the corresponding autocorrelation trace of the soliton. The conventional soliton sidebands are clearly visible on the soliton spectrum. Based on the autocorrelation trace, we determined that the soliton had a pulse width of about 933fs if a  $\text{sech}^2$  profile is assumed. Figure 2(b) is the RF spectrum of the soliton pulse train measured after passing through an external linear polarizer. No PEF was observed on the RF spectrum even when the orientation of the polarizer was randomly rotated.

In our experiment it was also noticed that depending on the orientation of the paddles of the polarization controller, GVLVSs other than those reported by Cundiff et al. could also be obtained. Figure 3(a) shows the optical spectrum of one of those vector solitons. On its optical spectrum apart from the so-called polarization sidebands [6], two sets of soliton sidebands were observed. Slightly changing the orientations of the paddles of the polarization controller shifted the separation of the two sets of sidebands as well as the central wavelength of the soliton spectrum. To examine the formation mechanism of the extra set of spectral sidebands, we further measured the optical spectrum of the soliton along each of the two orthogonal birefringence axes of the cavity. Our measurement procedure was as the following: we let the output of the laser pass through an external linear polarizer, through orienting the polarizer we first determined the direction of maximum pulse intensity transmission, and recorded the optical spectrum of the pulses along the polarization direction. Starting from the polarizer direction we then rotated the polarizer by  $90^\circ$  and recorded the soliton spectrum along the orthogonal polarization direction. After the polarization resolved measurement of the soliton spectrum, it turned out that the soliton components along each of the two orthogonal directions have much different central frequencies. Solitons along one polarization direction form one set of soliton sidebands. As shown in Fig. 3(a), one set of sidebands disappeared in the polarization resolved spectra, and the separation between the two sets of sidebands is exactly the soliton central frequency shift. Figure 3(b) shows the corresponding RF spectrum of Fig. 3(a). Again no PEF was observed on the RF spectrum even when the orientation of the

polarizer was randomly rotated. As except the amplitude change similar RF spectra was observed for the three measurement cases, we have only shown the one measured after passing through the external polarizer (0 degree).

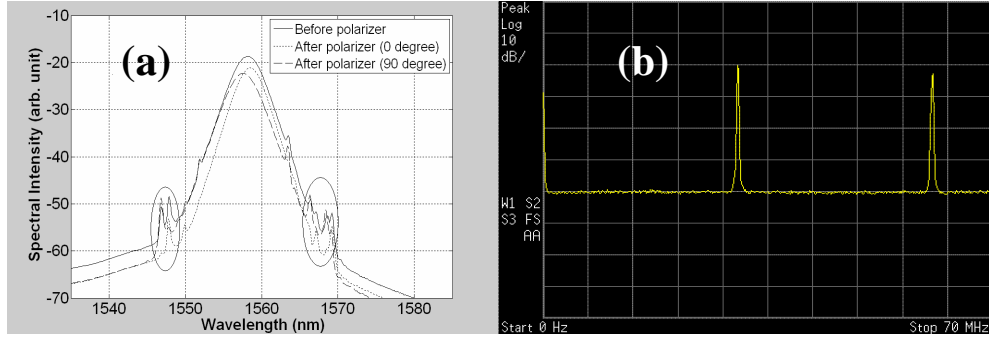


Fig. 3. The experimentally obtained vector soliton with soliton trapping: (a) Optical spectrum; (b) RF spectrum after an external linear polarizer.

#### 4. Numerical simulations

To verify our experimental observation, we further numerically simulated the laser operation based on the coupled Ginzburg-Landau equations and the pulse tracing technique described in [9]. In our model the light propagation in the birefringent fibers is governed by:

$$\begin{cases} \frac{\partial u}{\partial z} = i\beta u - \delta \frac{\partial u}{\partial t} - \frac{ik''}{2} \frac{\partial^2 u}{\partial t^2} + \frac{ik'''}{6} \frac{\partial^3 u}{\partial t^3} + i\gamma(|u|^2 + \frac{2}{3}|v|^2)u + \frac{i\gamma}{3}v^2u^* + \frac{g}{2}u + \frac{g}{2\Omega_g^2} \frac{\partial^2 u}{\partial t^2} \\ \frac{\partial v}{\partial z} = -i\beta v + \delta \frac{\partial v}{\partial t} - \frac{ik''}{2} \frac{\partial^2 v}{\partial t^2} + \frac{ik'''}{6} \frac{\partial^3 v}{\partial t^3} + i\gamma(|v|^2 + \frac{2}{3}|u|^2)v + \frac{i\gamma}{3}u^2v^* + \frac{g}{2}v + \frac{g}{2\Omega_g^2} \frac{\partial^2 v}{\partial t^2} \end{cases} \quad (1)$$

where  $u$  and  $v$  are the normalized envelopes of the optical pulses along the two orthogonal polarized modes of the optical fiber.  $2\beta = 2\pi\Delta n/\lambda$  is the wave-number difference between the two modes.  $2\delta = 2\beta\lambda/2\pi c$  is the inverse group velocity difference.  $k''$  is the second order dispersion coefficient,  $k'''$  is the third order dispersion coefficient and  $\gamma$  represents the nonlinearity of the fiber.  $g$  is the saturable gain coefficient of the fiber and  $\Omega_g$  is the bandwidth of the laser gain. For undoped fibers  $g = 0$ ; For erbium doped fiber, we considered its gain saturation as

$$g = G \exp\left[-\frac{\int (|u|^2 + |v|^2) dt}{P_{sat}}\right] \quad (2)$$

where  $G$  is the small signal gain coefficient and  $P_{sat}$  is the normalized saturation energy.

The absorption of the SESAM was described by the rate equation [10]:

$$\frac{\partial l_s}{\partial t} = -\frac{l_s - l_0}{T_{rec}} - \frac{|u|^2 + |v|^2}{E_{sat}} l_s \quad (3)$$

where  $T_{rec}$  is the absorption recovery time,  $I_0$  is the initial saturable absorption of the SESAM and  $E_{sat}$  is the absorber saturation energy.

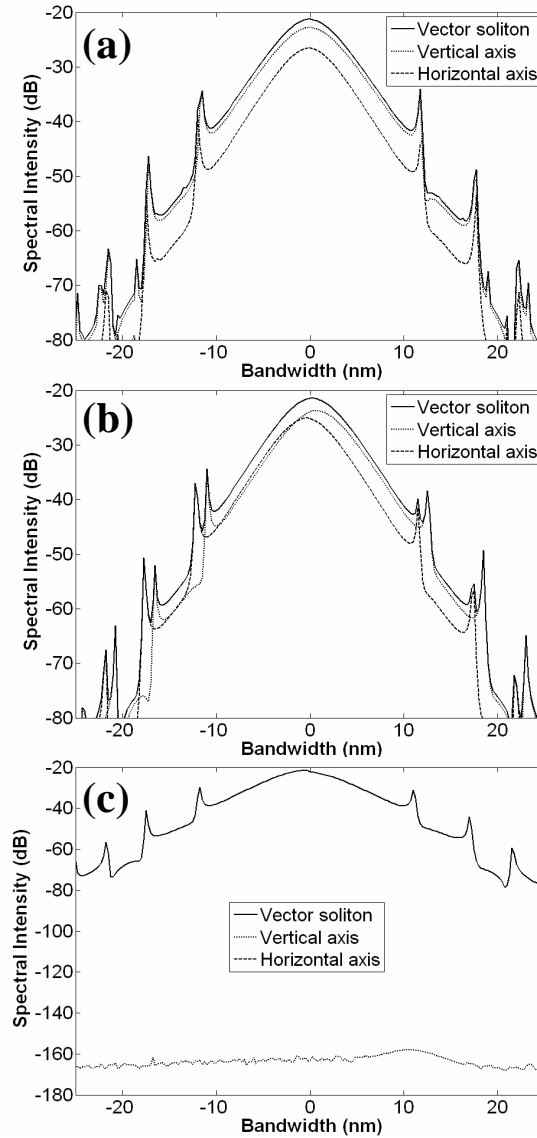


Fig. 4. The optical spectrum of the numerically obtained vector soliton with same parameters except that (a)  $L_b=L/2$ ; (b)  $L_b=L/20$ ; (c)  $L_b=L/200$ .

We used the following parameters:  $\gamma=3 \text{ W}^{-1}\text{km}^{-1}$ ,  $\Omega_g = 24 \text{ nm}$ ,  $P_{sat} = 100 \text{ pJ}$ ,  $k_{SMF}'' = -23 \text{ ps}^2/\text{km}$ ,  $k_{EDF}'' = -13 \text{ ps}^2/\text{km}$ ,  $k''' = -0.13 \text{ ps}^3/\text{km}$ ,  $E_{sat} = 1 \text{ pJ}$ ,  $I_0 = 0.15$ ,  $T_{rec} = 6 \text{ ps}$  and the cavity length  $L=6.4 \text{ m}$ . Numerically we found that when  $G=75$  stable mode locked pulses could be obtained, and determined by the net cavity birefringence, the mode-locked pulses could have different optical spectra. Figure 4 shows the optical spectrum of the stable pulses when the cavity beat length was selected as a)  $L_b=L/2$ , b)  $L_b=L/20$ , and c)  $L_b=L/200$ , respectively. When the cavity birefringence is small, for example  $L_b=L/2$ , the solitons formed along the two

orthogonal polarization directions have only slight central wavelength shift. Consequently, no double sets of soliton sidebands could be observed. While as the cavity birefringence becomes large, e.g.  $L_b=L/20$ , the central wavelength shift between the solitons is obvious. The solitons along each of the polarization directions generates its own soliton sidebands, therefore, resulting in double sets of solitons sidebands on the vector soliton spectrum. When the birefringence of the cavity is too strong, the stable solitons formed are linearly polarized along one polarization direction.

## 5. Discussion

Enlightened by the numerical simulations, our experimental results can be easily explained. Rotating the paddles of the polarization controller physically corresponds to changing the linear cavity birefringence. Therefore, both the PLVSSs and the GVLVSSs could be observed in the laser. In particular, for a GVLVSS, depending on the net cavity birefringence the two coupled solitons could have very different central frequencies and pulse energy, which leads to that the positions and amplitudes of their soliton sidebands are also different. Therefore, on the vector soliton spectrum there exist two sets of soliton sidebands.

Our experiments and numerical simulations clearly demonstrated the dependence of soliton central frequency difference between the two orthogonal soliton polarization components on the cavity birefringence. This result suggested again that the GVLVSS was formed through the soliton frequency shift of the coupled solitons. As the solitons formed in a laser are dissipative soliton, it furthermore demonstrates that soliton trapping effect is valid even for the dissipative solitons.

Finally, we note that the experimentally observed double sidebands are more obvious at the short wavelength side of the vector soliton spectrum, while in the simulations it is obvious at both wavelength sides. We believe that could be caused by the imperfect approximation made in our model as we have taken the parabolic gain approximation in our simulations. Therefore, nearly symmetric sidebands along the two birefringence axes were numerically obtained, while the experimentally observed sidebands have different amplitude due to the asymmetric gain of the real EDF. In addition, rotating the paddles of the polarization controller only changes the birefringence locally while in the simulation we have varies the total cavity birefringence. Nevertheless, the numerical simulations have well reproduced the experimental observations.

## 6. Conclusion

In conclusion, we have reported experimental observation of soliton trapping in a fiber laser mode-locked by a SESAM. We have shown that even under moderate linear cavity birefringence GVLVSSs could be formed in a fiber laser. Especially, due to that the coupled solitons have large different central frequencies and strength, and each of them forms its own soliton sidebands when circulating in the laser cavity, two sets of soliton sidebands could be observed on the vector soliton spectrum. Although the solitons formed in a laser are dissipative in nature, our experimental results show that they still have soliton trapping effect, indicating that soliton trapping could be a generic feature of all coupled solitary waves.

## Acknowledgment

This project is supported by the National Research Foundation Singapore under the contract NRF-G-CRP 2007-01.